Alpha cell MHC-I expression recruits cytotoxic CD8$^+$ T cells during human aging and type 2 diabetes.

Michael Schleh[1], Jean-Philippe Cartailler[2], Shristi Shrestha[2], Amanda Cambraia[1], Aliyah Habashy[1], Cara Ellis[3], Melanie Cutler[1], Gabriel Ferguson[1], Ricki Colman[4,5], Alvin Powers[6], Rafael Arrojo e Drigo[1,6,7,8*]

[1] Department of Molecular Physiology and Biophysics, Vanderbilt University School of Medicine, Nashville, TN
[2] Creative Data Solutions, Vanderbilt University School of Medicine, Nashville, TN
[3] Alberta Diabetes Institute and Department of Pharmacology, University of Alberta, Edmonton, Canada
[4] University of Wisconsin, Cell and Regenerative Biology, School of Medicine and Public Health, Madison, Wisconsin
[5] Wisconsin National Primate Research Center (WNPRC), Madison, Wisconsin
[6] Vanderbilt Diabetes Research and Training Center, Vanderbilt University Medical Center, Nashville, TN
[7] Center for Cell Systems Biology, Vanderbilt University School of Medicine, Nashville, TN
[8] Mass Spectrometry Research Center, Vanderbilt University School of Medicine, Nashville, TN
*Corresponding author

Keywords: aging, alpha cells, antigen presentation, calorie restriction, T cells

Address of Correspondence:
Rafael Arrojo e Drigo
718 Light Hall
2215 Garland Ave
Nashville, Tennessee 37232
r.drigo@vanderbilt.edu

Running Title: Alpha cell inflammation and calorie restriction in aging

Abstract

Aging is a major risk factor for type 2 diabetes (T2D), driven in part by loss of beta cell identity and function due to stress and islet inflammation. Calorie restriction (CR) improves metabolic health by promoting beta cell longevity in young animals. It remains unknown whether CR reverses cellular aging and dampens islet inflammation in aged animals. We show that aging alpha cells have an active inflammatory phenotype with increased IFNα/γ signaling that activates major histocompatibility complex (MHC-I) expression to promote $CD8^+$ T-cell accumulation in mouse and human islets. During human T2D, aging islet-resident $CD8^+$ T cells transition from memory states to activated effector phenotypes. Moreover, CR dampens alpha cell MHC-I expression to suppress $CD8^+$ cytotoxicity, which is sufficient to prevent islet inflammation and fibrosis in mice and non-human primates. Together, these findings highlight alpha cell MHC-I within the islet endocrine–immune axis in aging that may underlie fibrosis and disease development.

Introduction

Aging is a major risk factor for type 2 diabetes (T2D), affecting 29.2% of adults 65 and older in the United States[1]. Age-related deterioration in glycemic control has been traditionally attributed to declining peripheral insulin sensitivity, reduced beta cell insulin secretion, and increased hepatic insulin clearance[2-4]. However, older individuals also exhibit elevated circulating glucagon levels at basal and after a mixed meal stimulation[2], thus supporting the idea that dysregulation of alpha cell function may contribute to impaired glucose homeostasis during aging. Notably, hyperglucagonemia is a hallmark of adult T2D due to blunted glucose-dependent suppression of alpha cell glucose secretion[5] and elevated amino acid induced-glucagon release[6,7]. Notably, this phenotype is prevalent in older adults with impaired glucose tolerance and may be absent in T2D children[8], which suggests that aging alpha cells could be more likely to failure during T2D. Alpha and beta cells are long-lived endocrine cells that secrete insulin and glucagon, and constitute the majority of the islet[9], and are essential regulators of glucose homeostasis that must maintain function and support throughout the lifetime[10-12]. Aging beta cells have compromised structure-function due to loss of cellular identity markers, increased DNA damage and senescence, endoplasmic reticulum (ER) stress, compromised calcium homeostasis, impaired autophagy, increased transcriptional noise, amyloid deposition, and islet fibrosis[2,13-16]. It remains unknown if and how aging impacts alpha cell structure-function and glucagon-regulatory mechanisms.

Calorie restriction (CR) is a well-established dietary intervention that extends life- and health-spans across species, by delaying the onset of age-related cell dysfunction and disease[17-20]. Moderate reductions in energy intake (10–40%) improve metabolic homeostasis in both young and aged animal, whereas more severe restriction can lead to muscle wasting and immunosuppression[21]. At the molecular level, CR modulates major nutrient-sensing pathways including suppression of insulin-IGF1 signaling[22], inhibition of mammalian target of rapamycin complex (mTORC1) activity and activation of AMPK[23], reduction of oxidative stress and inflammatory tone[24], and enhanced autophagy[25,26]. Pharmacological strategies targeting these pathways, such as rapamycin (mTORC1 inhibition)[27], metformin (AMPK activation)[28], or resveratrol[29] have shown promises, but are limited by off-target effects, including immunosuppression and beta cell failure[30,31], which restricts their translational potential. CR and CR-mimicking interventions (i.e., intermittent fasting and time restricted feeding) in young adult mice promotes beta cell health, function, and longevity by enhancing peripheral insulin sensitivity that in turn reduces the metabolic demand for beta cell insulin secretion[32-35]. These pro-longevity effects are associated with increased expression of beta cell identity and circadian gene expression regulators, improved autophagy and protein homeostasis, mitochondrial homeostasis and ATP production, and reduced beta cell DNA damage and senescence[32-35]. Whether CR can rescue pancreatic inflammation and beta cell dysfunction in aging animals, and whether CR has any significant impact on aging alpha cells remains unclear.

To address these gaps, we integrated large-scale meta-analyses of publicly available human islet proteomic, transcriptomic, and spatial proteomic datasets to define molecular signatures of aging in non-diabetic (ND) donors, and to determine whether these cellular signatures translate to T2D. We then used CR in aged mice to translate whether dietary restriction can reverse age-associated cellular and molecular alterations in old islets. As expected, the aging human islet proteome exhibited increased ER stress, senescence, and beta cell immaturity signatures. Surprisingly, we also observed heightened inflammatory markers linked to innate immunity, coupled with adaptive immunity in antigen presentation markers. Single-cell transcriptomics revealed these proteomic signatures were largely explained by upregulation of hallmark inflammation genes in aging alpha cells, including activation of MHC-I genes and interferon (IFN) α/γ pathways. Using transcription factor inference algorithms, we found activation of alpha cell

inflammatory signatures is attributed to activation of pro-inflammatory transcription factors (TFs) KLF6, IRF1, and NFKB1. Multiplexed spatial mass spectrometry confirmed higher MHC-I (HLA-ABC) expression in aging alpha cells, but not beta cells, and revealed an age-related increase in central memory ($CD27^+CD45RA^-$) $CD8^+$ T cells ($CD8_{CM}$) that shifted toward a terminally differentiated effector memory phenotype ($CD27^-CD45RA^+$; $CD8_{TEM}$) in T2D islets. Exposure of aged lean mice to 20% CR for two months significantly reduced alpha cell pro-inflammatory gene expression and disrupted ligand-receptor inference of alpha-to-T-cell communication, suggesting that CR broadly attenuates immune activation through the suppression of alpha cell inflammatory signaling. Together, our findings indicate that aging alpha cells exhibit pro-inflammatory signatures that underlie age-related pancreas inflammation and fibrosis via infiltration of cytotoxic $CD8^+$ T cells. These aspects are conserved in mice and humans and is suppressed by CR in mouse and non-human primates (NHPs). Therefore, CR may offer the dual benefit of improving overall metabolic health in lean aging organisms while reversing islet inflammation signatures associated with impaired beta cell function and compromised glucose homeostasis.

Results

Aging ND islets heighten inflammatory and T-cell receptor activation pathways with mTORC1 and heightened unfolded protein response. Islet inflammation and fibrosis are recognized hallmarks of human pancreas aging and diabetes, contributing to beta cell functional decline[36-38]. To define human proteomic aging signatures, we leveraged a comprehensive human islet proteomics dataset generated by the HumanIslets consortium (**Figure 1A, Supplementary Table 1**)[39,40]. Comparisons of young (28±4 years, n=26) and old (71±3 years, n=19) ND adults identified 86 proteins significantly increased by aging and 17 proteins decreased. Reactome pathway enrichment revealed increased immune regulatory and innate immune pathways, amino acid metabolism and mTORC1-related metabolic factors, and ER stress in old islets (**Figure 1B**). These age-associated changes included elevated beta cell immaturity markers (RBP4[41]; **Figure 1C**), senescence (CDKN1A/p21[42], **Figure 1D**), ER stress signaling (ATF6, CHOP, and PERK; **Figure 1E**), and increased mTORC1 activation proteins (LAMP2, LAMTOR, RAGA, RAGC; **Figure 1F**). Moreover, we observed a robust immune activation signature characterized by increased expression of pro-inflammatory and antigen presentation proteins, including the MHC-1 antigen, HLA-A, T-cell receptor (TCR) signaling and memory components such as CD28 and CD44, and additional antigen processing and immune-regulatory signaling (TGF-β1, TOM1, and SLC15A4; **Figure 1G**). Together, these findings reinforce previous reports to support that aging human islets have an active cellular stress response accompanied by enhanced inflammatory signaling to upregulate immune cell activation and recruitment, although the cell-type–specific distinctions to these processes remain to be defined.

Single cell transcriptomics reveal activation of inflammatory signaling in aging human alpha cells. Over the past decade, several groups have applied diverse single cell transcriptomic approaches to investigate how islet cell gene expression and chromatin accessibility are regulated during development, aging, and diabetes[41,43-52]. We recently demonstrated that aging ND beta cells have an active ER stress response[43], which explains the higher level of ER stress markers in bulk islet proteome (**Figure 1**). In mice, a recent bulk RNA-seq study of sorted alpha cells, beta cells, and delta cells associated aging with the activation of immune responses and MHC-I complex gene expression[53]. To identify the specific islet cell types contributing to the increased expression of pro-inflammatory markers identified in the human islet proteomics (including MHC-I), we performed meta-analysis of single cell mRNA sequencing (scRNA-seq) transcriptomics deposited in the HPAP PANC-DB database[54-57]. We initially curated scRNA-seq data from a total of n=132 donor samples and applied a comprehensive bioinformatics approach to filter samples and perform robust quality control and covariate correction for sex, BMI, ethnicity, sequencing chemistry, and sequencing batch (see methods for details) (**Figure 2A**,

Supplementary Figure 1A-B, **Supplementary Table 2**). This resulted in a final dataset containing scRNA-seq profiles from n=32 donors (131,610 annotated islet cells, including 56,851 alpha cells), stratified into young adults (20-40 years of age) and old adults (≥50 years of age) (**Figure 2B**).

First, we investigated which ND human islet cell types express immune signaling genes and found that alpha cells exhibit the highest expression of HLA-ABC antigens, which encode the MHC-1 complex, among all major endocrine cell types – which is followed by endothelial and actual immune cell types (**Figure 2C**). Pseudobulk differential gene expression and principal components analysis (PCA) resolved groups into distinct clusters (**Supplementary Figure 1B**). Gene Set Enrichment Analysis (GSEA) identified activation of both IFNα and IFNγ signaling (*STAT1*, *SOCS1*, *SOCS3*, *IRF7*, *IRF9*, *IL7*, and *IL15*; **Figure 2D-E**), and MHC-I-mediated antigen presentation pathways (*HLA-E*, *HLA-F*, and *TAP1*: **Figure 2F**) in old alpha cells. In addition, aging alpha cells had increased expression of genes associated with glucose, fatty acid, and amino acid catabolism (**Figure 2G-I**). These signatures correlated with activation of a "beta cell-like" senescence program marked (CDKN1A/p21, CDKN1B/p27, CDKN2A/p16, and IGF1R), and a lack of an active ER stress signature (**Supplementary Figure 1C**). To determine if these transcriptional changes correlate with alterations in alpha cell glucagon secretion, we analyzed HPAP human islet perifusion data from young and old donors from two different human islet analysis centers (UPenn and Vanderbilt), which used complementary stimulation protocols to test for the effect of several insulin and glucagon secretagogues. This revealed that alpha cells from older donors have increased glucagon secretion in response to stimulation with a mixed amino acid (AA) cocktail and to de-polarization with KCL (**Figure 2J**). No changes were observed when alpha cells were stimulated with low glucose, high glucose, and epinephrine (**Supplementary Figure 1D**). Together, these results indicate that aging human alpha cells acquire senescence-associated features, display heightened AA catabolism and AA-dependent glucagon secretion, and an active IFN signaling and MHC-I antigen-presentation programs.

Re-organization of gene regulatory networks activates inflammatory gene expression in aging alpha cells. We previously applied the transcription factor (TF) inference algorithm pySCENIC[58] to show that aging beta cell stress arises from reconfigured gene regulatory networks (GRNs) and activation of stress TFs[43]. Here, we used pySCENIC and graph network analysis to characterize GRNs in aging alpha cells and identify TFs driving inflammation. Reconstruction of GRNs in young and old alpha cells revealed canonical alpha cell TFs (ARX, PAX6, and MAFB) (**Figure 3A-B**). Young alpha cells presented few TFs forming small regulons, composed of a limited number of TFs, including regulators previously implicated in beta cell GRNs (MAFA, EGR1, and BCLAF1; **Figure 3A**). In contrast, aging alpha cells exhibited expanded GRNs connected to pro-inflammatory TFs such as KLF6, NFKB1, IRF1, and MXD1, consistent with enrichment of their downstream targets in older alpha cells (**Figure 3B-D**).

We previously found that TFs maintaining beta cell identity in young adults can be "redirected" to activate cell stress and beta cell dedifferentiation programs during aging[43]. To investigate if a similar mechanism was in place in aging alpha cells, we analyzed the identity of TF regulons linked to NFKB1, KLF6, IRF1, and MAFB in young versus old alpha cells. This approach revealed substantial shifts in TF regulon identity, including the activation of a KLF6 regulon with 226 target genes not expressed in young alpha cells, and expansion of NFKB1, IRF1, and MAFB regulons (**Figure 3C-D**). Reactome Pathway analysis[59] mapped these regulons to inflammatory pathways, including immune activation and cytokine signaling (i.e., IFN, IL20, IL4, and IL13), caspase-mediated cell death, MAPK and TGF-β signaling, and response to mechanical stress (**Figure 3E-F, Supplementary Figure 2A**). Notably, HNF1A and MAFB regulons in aging alpha cells were associated with ERBB4 signaling, which mediates epidermal growth factor (EGF) receptor signaling cascades[60].

To identify potential activators of these inflammatory pathways, we applied CellChat[61] to infer cell-cell communication from scRNA-seq data across young and old islet cell types (**Figure 2G-I**). This approach identified 74 signaling pathways that are significantly up regulated in aging human alpha cells (**Supplementary Figure 2B, Supplementary Table 3**). These enriched pathways were further categorized into major molecular classes such as extracellular matrix (ECM) adhesion (Laminin, collagen, Vcam/Icam) and remodeling (Mmp), growth factors (Fgf, Egf, Pdgf), GPCR signaling (Adgrl, Prostaglandins), immune checkpoints (Lair1, MHC-I, Cd46, IL6), neurotransmitters and other hormones (Gaba-b, Insulin, ApoE), Semaphorins (Sema3), membrane receptor signaling (Wnt, Tgfb, App), tight junctions (Ocln, Clnd), and "other" (Ptprm, annexin). Approximately 30% of enriched pathways involved ECM biology, reflecting the fibrotic aging islet microenvironment[37], (**Figure 3G**, **Supplementary Figure 2B-C**). Growth factor pathways, including pro-fibrotic factor TGFB1 were the second most represented (**Figure 3H, Supplementary Figure 2D-E and 3A**). Beta cells were primary TGFB1 secretory source in both young and old islets, followed by quiescent stellate and ductal cells. In young islets, TGFB1 signaling from both alpha and beta cells targeted macrophages, T cells, endothelial cells, and activated stellate cells; in older islets, signaling expanded to acinar and quiescent microglia-like cells (**Figure 3H**). Strikingly, alpha and beta cells established WNT signaling networks and activated stellate and acinar cells communicated via LIF – two molecules that are involved in TGFB1-mediated fibrosis (**Supplementary Figure 3A**)[62,63]. FGF signaling from ductal, activated stellate, and microglia cells primarily targeted aging alpha cells, whereas EGF and GDF signaling were mostly restricted to the extra-islet compartment (**Figure 3H, Supplementary Figure 2D-3 and 3A**). Older alpha cells were enriched in immune signaling, including CD46 (amplifying $CD8^+$ T-cell signaling[64] and $CD4/8^+$ IFNγ production[65]), prostaglandin and IL6 signaling (which regulates alpha cell secretory function[66]), and protein tyrosine phosphatase receptor (PRPRM), a modulatory of IL6 signaling during stress responses[67] (**Figure 3I, Supplementary Figure 2F and 3A**). Together, these studies highlight aging human alpha cells acquire a pro-inflammatory identity through extensive rewiring of their GRNs, marked by activation of stress- and cytokine-responsive TFs (including IRF1, NFKB1, and KLF6) and reduced MAFB activity. These regulons appear to be amplified by TGFB1-, WNT-, and T-cell- and cytokine-mediated signaling from neighboring islet and stromal cells, processes that may contribute to the fibrotic remodeling of the aging islet microenvironment.

Spatial analysis of aging human pancreases identifies alpha-T-cell interactions *in situ*. Aging ND human pancreases exhibit multiple features of chronic low-grade inflammation, including increased fibrosis, higher incidence of acinar-to-ductal metaplasia (ADM), angiopathy, and pancreatic adiposity[38]. To validate our bulk proteomic and scRNA-seq findings *in situ*, we analyzed high-dimensional imaging mass cytometry (IMC) and CO-Detection by indexing (CODEX) datasets from HPAP[56,57]. Human ND pancreas samples were stratified into young adult (22-40 years) and old adults (47-58 years) groups (**Figure 4A and 4D; Supplementary Figure 4B and 5B; Supplementary Tables 4 and 5**). Individual cells from each donor image were segmented using a custom QuPath-based and spatial analysis pipeline (see methods), enabling unsupervised clustering into major endocrine and immune cell populations based on marker expression ((**Supplementary Figure 4A, C-G and 5A, C-G**), including alpha (GCG^+), beta (C-$peptide^+$), delta (SST^+), pancreatic polypeptide (PP^+), endothelial cells ($CD31^+$), Epithelial/Acinar cells ($CK19^+/CA2^+$), M1-like macrophages ($CD45^+CD68^+CD163^-$) , M2-like macrophages ($CD45^+CD68^+CD163^+$), and T cells ($CD45^+CD3^+CD4^+$ and $CD45^+CD3^+CD8^+$) (**Figure 4B and 4E, Supplementary Tables 6 and 7**). This framework enabled spatial mapping of all major pancreatic and immune cell types in either IMC (**Figure 4C**) and CODEX (**Figure 4F**) platforms, as well as quantification of immune and endocrine cell phenotyping **(Figure 4G-H**; **Supplementary Figure 6A and 6C**). Notably, aging pancreases showed significant expansion of $CD45^+CD3^+$ T

cells, predominantly driven by CD8$^+$ T-cell infiltration (**Figure 4G-H, Supplementary Figure 6C**).

To investigate endocrine-immune interactions underlying CD8$^+$ T-cell expansion, we performed nearest-neighbor spatial analyses to quantify the proximity of CD8$^+$ T cells to their nearest alpha and beta cells. Aged pancreases displayed a higher proportion of alpha cells localized within close proximity (<50μm) to CD8$^+$ T cells (**Figure 4I**), a relationship not observed for beta cells (**Figure 4J**). No age-associated differences were detected between CD4$^+$ T cells to alpha cells or in total macrophage density (**Figure 4G-H**). Notably, the increased spatial proximity between alpha cells and CD8$^+$ T cells was accompanied with increased expression of HLA-ABC abundance (encoding MHC-I complex) and attenuated abundance of HLA-DR abundance (encoding MHC-II) in alpha cells, whereas beta cells showed no such change (**Figure 4K-M**). Importantly, we detected expected age-associated decreases in beta cell identity markers PDX-1, NKX6-1, and PAX-6[43] (**Supplementary Figure 6B**), confirming the classical aging beta cell phenotypes[38,43]. Together, these findings extend our isolated islet analyses by demonstrating that human islet and pancreatic aging is marked by increased pro-inflammatory signaling from alpha cells, which correlates with elevated CD8$^+$ T-cell density *in situ*. Given that MHC molecules present antigenic peptides to T cells via TCR engagement, these results suggest that alpha cell-intrinsic inflammatory pathways contribute to the immune activation and pancreatic inflammation that emerge with aging.

T2D expands pancreatic CD8$^+$ T cells that shift towards terminal effector-memory phenotypes. To determine whether whole-pancreas immune features associated with immune aging overlap with T2D, we analyzed additional CODEX data from T2D donors profiled through HPAP (**Supplementary Table 8**). These cohorts were matched for age and BMI; however, T2D donors displayed expected impairments in glycemia, evidenced by higher HbA1c and reduced C-peptide (**Figure 5A**). Integration of 942,724 single-cell profiles identified targeted endocrine (99,744 cells) and immune (195,140 cells) compartments (**Figure 5B**). Endocrine cell clustering identified two distinct beta cell populations: a CPEP$^+$CHGA$^+$ population and a CPEP$^+$CHGA$^+$COL4A1$^+$COL6$^+$ "fibrotic" beta cell state enriched in T2D (**Figure 5C**). These cells exhibited higher interaction with fibrotic ECM and thus were detected as being COL4A1$^+$COL6$^+$ by our cell segmentation algorithms. T2D beta cells were marked by lower CPEP, CHGA, NKX6-1, and Ki67 expression (**Figure 5D**), while alpha cells had attenuated SOX9 and Ki67 (**Figure 5E**), consistent with diminished endocrine cell identity and proliferative capacity. Within immune compartments, we observed a trend towards increased CD8$^+$ T-cell representation and decreased CD68$^+$CD163$^+$ M2-like macrophages (**Figure 5F**), accompanied by a significant ~2-fold increase in pancreas CD8$^+$ T-cell density (**Figure 5G**). Together, these findings demonstrate that T2D amplifies CD8$^+$ T-cell density, mirroring patterns observed in aging and establishes heightened cytotoxic pressure within the pancreas.

To resolve whether the increased adaptive immune phenotype observed in the aging and T2D pancreas was localized within islets, we analyzed HPAP cytometry by time-of-flight (CyTOF) data from isolated islets of young (26 ± 8 years, n=13), old (54 ± 5 years, n=14), and T2D (50 ± 8 years, n=13) human donors (**Figure 5H, Supplementary Table 9**). Both aging and T2D presented greater CD45$^+$ live immune cell abundance compared with young adults, corresponding with to higher frequencies of islet CD3$^+$CD8$^+$ T cells within the CD45$^+$ immune compartment (**Figure 5I-J**). CD8$^+$ T cells differentiate along a spectrum from naïve (CD8$_{naïve}$) to CD8$_{CM}$ and CD8$_{TEM}$ states in response to TCR activation by antigen and cytokine stimulation. In T2D islets, we observed a reduction in CD45RA$^+$CD27$^+$ CD8$_{naïve}$ T cells compared with young adults, whereas aging increased CD45RA$^-$CD27$^+$ CD8$_{CM}$ T cells (**Figure 5K-L**). T2D islets further shifted CD8$^+$ T-cell populations towards a higher CD45RA$^+$CD27$^-$ CD8$_{TEM}$ phenotype, resulting in elevated effector-to-central memory ratio that was not observed in aging ND samples

306 (**Figure 5L-M**). Together, these data show that T2D intensifies pancreas and islet CD8$^+$ T-cell
307 infiltration and drives their progression toward terminal effector-memory states, establishing a
308 cytotoxic immune milieu that is distinct from, but overlaps with immune aging.

309 **Calorie restriction improves glucose tolerance and dampens alpha cell inflammation in**
310 **mice.** Dieting through calorie restriction (CR) and weight loss interventions is commonly pre-
311 scribed as an initial strategy to normalize glycemia in individuals with prediabetes and T2D. We
312 and others have shown that CR enhances glucose homeostasis and delays the onset of inflam-
313 mation and aging hallmarks associated with metabolic dysfunction, including in beta cells[68-72].
314 Therefore, we tested whether CR could reverse aging signatures in alpha and beta cells *in vivo*.
315 To achieve this, 72-week-old C57BL/6J male mice were subjected to a 2-month, 20% CR feed-
316 ing regimen, while age-matched controls remained on ad-libitum (AL) diet (**Figure 6A**). As ex-
317 pected, CR mice consumed 80% of total kcal intake compared to AL-fed controls (**Supplemen-**
318 **tary Figure 7A-B**). This intervention induced a steady decline in body weight over 2 months, re-
319 sulting in ~12% weight loss (**Figure 6B, Supplementary Figure 7C-D**), which was due to a pre-
320 dominant loss in fat mass. Tissue-specific weight loss was also observed in the liver and epidid-
321 ymal white adipose tissue (eWAT) of CR mice (**Supplementary Figure 7E-H**). Metabolic pheno-
322 typing and behavioral analysis revealed comparable overall energy expenditure and oxygen
323 consumption between AL and CR mice (**Supplementary Figure 7I-L**). However, carbon dioxide
324 production and carbohydrate oxidation were higher in CR mice during the dark period, when
325 food was available (**Supplementary Figure 7M-P**), indicating a higher preference for carbohy-
326 drate metabolism in CR mice during active feeding periods and a rapid shift towards fatty acid
327 metabolism during inactivity and food withdrawal. To assess how CR influences glucose homeo-
328 stasis in aged mice, we performed mixed meal tolerance tests (MTTs; 2 g glucose/kg body
329 weight, Ensure Original). Baseline MTTs were conducted at 72 weeks, prior to CR. After 2
330 months of CR, old mice exhibited significantly improved glucose tolerance at 80 weeks, at-
331 tributed to enhanced insulin sensitivity (**Figure 6C**). This improvement was accompanied by
332 ~50% reductions in fasting and glucose-stimulated beta cell insulin secretion (**Supplementary**
333 **Figure 7Q**). Similar to younger CR-treated mice[32], CR preserved beta cell function in aged mice
334 by reducing the relative insulin secretory demand required to maintain normoglycemia, demon-
335 strating that CR-mediated functional beta cell adaptation remains intact in aging (**Supplemen-**
336 **tary Figure 7R**).

337 We previously showed that CR modulates beta cell heterogeneity by activating pro-lon-
338 gevity and homeostasis pathways that enhance beta cell protein and organelle quality-control
339 mechanisms[32]. This transcriptional response is driven by the activation of TF-directed GRNs
340 that increase the expression of beta cell identity and longevity genes[32]. To determine whether
341 CR elicits similar adaptative programs to old beta cells during CR, we performed single nucleus
342 RNA sequencing (snRNA-seq, 10X genomics) on islet nuclei isolated from AL and CR-fed mice
343 (**Figure 6A**). A total of 32,380 cells were sequenced (AL=17,344, CR=15,306) to identify all ma-
344 jor islet cell types, including beta cells (*Ins1*, *Ins2*, and *Ero1b*), alpha cells (*Gcg*), delta cells
345 (*Sst*), endothelial cells (*Pecam1*), and pancreatic polypeptide cells (*Ppy*) (**Figure 6D-E, Supple-**
346 **mentary Figure 8A**). Approximately 65% of the sequenced cells were beta cells, and CR did
347 not impact the relative composition of the heterogeneous beta cell population or islet cytoarchi-
348 tecture composition (**Supplementary Figure 8B-H**). Using pseudobulk analysis of beta cells fol-
349 lowed by KEGG and STRING pathways analysis, we observed a narrow range of CR-mediated
350 effects on beta cell gene expression, limited to downregulation of few ER protein processing
351 and folding (*Hspa1a/b/HSP70, Hspa8, Hsp90ab1, Dnaja1/HSP40, and Calr)*, cell stress (*Ypel2*,
352 *Txnip*), and insulin synthesis (*Ins1*) genes (**Figure 6F and Supplementary Figure 6D-J**). These
353 data indicate that beta cell functional adaptation to CR in aging mice primarily reflects compen-
354 sation for age-related proteostatic stress from insulin production.

355 Remarkably, CR exerted a stronger transcriptional effect on alpha cells, modulating
356 nearly five times more genes than beta cells (184 vs. 36 differentially expressed genes; **Figure**
357 **6F**). Differential gene expression and pathway enrichment analyses of old CR alpha cell gene
358 signatures revealed upregulation of pathways associated with glucagon, glucose and fatty acid
359 metabolism (*Gcg, Gys2, and Acacb*) and Pgc1a (*Ppargc1a)* (**Figure 6G**). In contrast, CR sup-
360 pressed 159 genes involved in immune signaling, including pathways related to TCR signaling,
361 antigen presentation, and immune cell recruitment pathways (*Cd44, Cd28, Il7r, Il18r1, and Ccr7;*
362 **Figure 6H**). This included genes involved in cell-cell signaling via MHC class I (*H2-Q7*, *H2-Q6*,
363 *H2-K1*) and MHC class II (*H2-Aa*, *H2-Ab1*, *H2-Ob*) antigens **(Figure 6H-I)**. These findings
364 demonstrate that 2 months of mild CR reduces age-associated pro-inflammatory signaling in ag-
365 ing alpha cells, thus further supporting an immunoregulatory role for alpha cells during aging[53]
366 (Figures 2-4) and type 1 diabetes[73].

367 **CR suppresses alpha cell immune signaling to reduce islet inflammation.** To further
368 investigate how CR-mediated modulation of aging alpha cell inflammatory gene expression in-
369 fluences the cellular and molecular profile of islet immune cells, we quantified the relative com-
370 position and transcriptional signatures immune cell types identified by snRNA-seq (**Figure 7A**).
371 This revealed a significant decrease in B cells, T cells, proliferating B cells, and antigen present-
372 ing cells (APCs) in CR mouse islets, whereas the relative density and transcriptional profile of
373 islet-resident macrophages were unchanged (**Figure 7B**). Furthermore, old CR mouse islets
374 had a marked reduction in islet T cells, including a near total ablation of cytotoxic $CD8^+$ effector
375 T cells (**Figure 7C-D**). Here, the remaining $CD8^+$ T cells in CR islets had reduced expression of
376 effector markers granzyme K (*Gzmk*), IL-2 receptor (Il2ra/*Cd25*), Ccr7, and *Txk*; all markers of
377 activated T cells (**Figure 7E**). We validated these changes *in situ* using immunohistochemistry
378 and confocal microscopy of AL and CR old pancreases, followed by spatial mapping of alpha
379 cells, beta cells, and $CD3^+$ T cells (**Figure 7F)**. This approach revealed a significant reduction in
380 T-cell density (**Figure 7G**), and increased distance between T cells and alpha cells (**Figure 7H**).
381 These data support recent findings of immune cell infiltration in the aging mouse islet[61] and
382 demonstrate that CR modulates the recruitment of $Cd8^+$ T cells to the islet by reducing their
383 preferential proximity to old alpha cells.

384 To identify communication pathways linking aged alpha cells with $CD8^+$ T cells and their
385 modulation by CR, we performed receptor-ligand inference analysis using CellChat[74,75] to recon-
386 struct cell-cell communication networks in AL and CR aging mouse islets (**Figure 7I**)[76]. This ap-
387 proach revealed an overall downregulation of intercellular communication between islet immune
388 cells and alpha cells, beta cells, and delta cells (**Figure 7I**). This was underscored by a signifi-
389 cant decrease in Cd45-based interactions between old alpha cells and T- and B-cells in CR
390 mice (**Figure 7J**). These data further supports the idea that old alpha cells are important signal-
391 ing hubs that communicate with effector adaptive immune cells, including cytotoxic $CD8^+$ T cells
392 that are associated with islet inflammation in aging and T2D (**Figures 2-5**).

393 Finally, we investigated whether CR had similar anti-inflammatory effects in the pancreas
394 of NHPs on AL or 30% CR for at least 17 years[77] (**Figure 7K**). Importantly, like our CR mouse
395 models (Figure 6-7 and[78]), CR NHPs were more insulin sensitive and had reduced beta cell in-
396 sulin release (**Figure 7K**). In humans, islet inflammation during aging is associated with in-
397 creased lipid droplet accumulation, islet and vascular fibrosis, and islet amyloid accumula-
398 tion[37,38]. Therefore, we ran a double-blind analysis to quantify the impact of CR on these tissue
399 signatures in the pancreases of age-matched AL and CR NHPs (see methods for details). We
400 found that CR significantly decreased pancreatic lipid droplet accumulation and islet fibrosis
401 (**Figure 7L-N**), suggesting an underlying inflammatory may contribute to fibrosis in aged NHPs
402 and can be rescued by CR.

These results indicate that CR profoundly reshapes the aging islet immune environment by suppressing alpha cell inflammatory and MHC-I signaling to reduce CD8$^+$ T-cell recruitment and cytotoxicity, while diminishing intercellular communication between alpha cells and adaptive immune cells. Moreover, the observation that long-term CR similarly attenuates inflammatory and fibrotic features in NHPs suggests that CR promotes healthier islet and pancreatic aging across species.

Discussion

Aging is associated with an active and low-grade inflammatory process in different tissues, where inflammation is a key signature of several age-associated degenerative and metabolic diseases, including Alzheimer's[79], and obesity and diabetes[80]. In the pancreas, aging is associated with increased islet macrophage infiltration and vascular fibrosis[37], and share other key hallmarks of T1D and T2D islet pathophysiology such as beta cell ER stress, compromised beta cell identity and function, and beta cell senescence[15,37,38,42-44,53,81-88]; however, recent studies have implicated the activation of inflammatory responses in human alpha cells during T1D and T2D[73,89].

In this manuscript, we identify activation of immune signaling and inflammation as a key signature of aging human islets from non-diabetic individuals. This phenotype is defined by active IFNγ signaling and MHC-I expression in old alpha cells, which is due to activation of IFNγ-responsive TFs IRF1, NFKB1, and KLF6. In addition, old human alpha cells appear to be more sensitive to amino-acid-dependent glucagon release, which could be explained by the observed increase in the expression of several AA catabolism enzymes. Moreover, our data shows that old alpha cells have increased immune signaling pathways (IL6, CD46), and that aging islets have increased TGFB1 levels (and of other growth factors like FGF and LIFR) that signal mostly from beta cells and that may act to promote and increase islet fibrosis. Importantly, activation of alpha cell immune signaling during aging translates into increased physical interactions between old alpha cells with cytotoxic CD8$^+$ T cells, which accumulate within the aging human islet microenvironment. Strikingly, most old islet CD8$^+$ cells have a "memory-like" phenotype (CD27$^+$), thus indicating that these cells have been exposed to T cell antigens. While our study does not identify which antigen is presented by alpha cell MHC-Is, a recent study where human islets were exposed to cytokine stress (e.g., IFNγ) identified several new MHC-I antigens, many of which are enriched in aging alpha cells (i.e., NFKB1, IRF9, TAP1, IFIT3, PSMB8, and STAT1)[81]. Importantly, while density of islet CD8+ cells is similar between non-diabetic and T2D islets, most T2D islet CD8+ cells have an effector-like signature (CD45RA$^+$ CD8$^+$). This data indicates that infiltration of CD8+ cells in aging human islets occurs independently of T2D and further suggests that islet inflammation in individuals with T2D onset during old age involves activation of alpha cell-interacting and "resident" CD8+ cells.

Calorie restriction (CR) prolongs the lifespan and health span of multiple organisms, from yeast to mice to non-human primates to humans[70-72,90-92]. The benefits of CR depend on CR-dependent improvements in glucose homeostasis mechanisms, including enhanced insulin sensitivity that reduces the metabolic demand for insulin release from beta cells[32,71,93,94]. Our experiments with 80-week-old mice on CR for 2 months demonstrate that the insulin-sensitizing and beta cell functional adaptation pathways promoted by CR are not impaired during aging, not that these involve significant transcriptional reorganization in the beta cell. This is likely explained by the limited plasticity of aging beta cells in response to metabolic challenges[95]. In contrast, CR acted on old alpha cells and significantly suppressed the expression of pro-inflammatory genes, including MHC-I and TCR signaling pathways. This CR-dependent modulation dampened CD45-mediated communication between immune cells and alpha cells, which was sufficient to reduce the density of T cells in aging islet periphery. Strikingly, a similar anti-

inflammatory effect was observed in NHPs kept on CR for most of their adult life, where CR prevented the accumulation of pancreatic lipid droplets, and of islet fibrosis amyloid deposition.

In conclusion, our findings identify the relationship between alpha cells and immune cells within the islet of Langerhans during aging that may underlie the onset of islet fibrosis and inflammation to promote T2D development during old age.

Data availability: IMC, CODEX, and human islet single cell RNAseq are available via PANC-DB (Zenodo: 10.5281/zenodo.15588155). Mouse snRNA-seq is readily and freely available at Zenodo and raw FASTQ data deposited at Gene Expression Omnibus.

Acknowledgements: We acknowledge the following Vanderbilt University (VU) and Vanderbilt University Medical Center (VUMC) core facilities: VUMC Hormone Assay & Analytical Services Core (NIH DK020593), VU Metabolic Mouse Phenotyping Center [VMMPC (NIH DK059637; www.vmmpc.org)], Translational Pathology Shared Resource (NCI/NIH Cancer Center Support Grant 5P30 CA68485-19), and Vanderbilt Technologies for Advanced Genomics (VANTAGE) core laboratory. VANTAGE is supported in part by Clinical and Translational Science Award Grant 5UL1 RR024975-03, Vanderbilt Ingram Cancer Center Grant P30 CA68485, Vanderbilt Vision Center Grant P30 EY08126, and National Institutes of Health/National Center for Research Resources Grant G20 RR030956. This manuscript used data acquired from the database (https://hpap.pmacs.upenn.edu/) of the Human Pancreas Analysis Program (HPAP; RRID:SCR_016202; and[56,57]). HPAP is part of a Human Islet Research Network (RRID:SCR_014393) consortium (UC4-DK112217, U01-DK123594, UC4-DK112232, and U01-DK123716). We would also like to acknowledge NIH grant R01AG040178. The WNPRC is supported by research facilities improvement programs NCRR/ORIP grants P51RR000167/P51OD011106. This work includes data and/or analyses from HumanIslets.com funded by the Canadian Institutes of Health Research, JDRF Canada, and Diabetes Canada (5-SRA-2021-1149-S-B/TG 179092) with data from islets isolated by the Alberta Diabetes Institute IsletCore with the support of the Human Organ Procurement and Exchange program, Trillium Gift of Life Network, BC Transplant, Quebec Transplant, and other Canadian organ procurement organizations with written informed donor consent as approved by the Human Research Ethics Board at the University of Alberta (Pro00013094). Finally, we would like to acknowledge Dr Patrick E MacDonald from ADI – Edmonton (Canada) for critical comments and inputs during data collection and manuscript writing stages of this project.

Funding: This work was support by the National Institutes of Health grants 1R01DK138141 awarded to R.A.D. M.S. is supported by the National Institutes of Health Molecular Endocrinology Training Program (T32DK007563).

Author Contributions: M.S., S.S., JP.C., R.C., and R.A.D designed experiments. M.S., A.C., M.C., G.F., S.S., JP.C., R.C., A.H., C.E., A.P., and R.A.D. collected data and assisted with data analysis and project management. M.S., S.S., JP.C., and R.A.D. completed data analysis. M.S. and R.A.D. interpreted data and wrote the manuscript.

Disclosures: The authors have nothing to disclose.

492 **REFERENCES**

493 1. National Diabetes Statistics Report. *Centers for Disease Control and Prevention* (2024).
494 2. Basu, R.*, et al.* Mechanisms of the age-associated deterioration in glucose tolerance:
495 contribution of alterations in insulin secretion, action, and clearance. *Diabetes* **52**, 1738-
496 1748 (2003).
497 3. Petersen, K.F.*, et al.* Mitochondrial dysfunction in the elderly: possible role in insulin
498 resistance. *Science* **300**, 1140-1142 (2003).
499 4. Cowie, C.C.*, et al.* Prevalence of diabetes and impaired fasting glucose in adults in the U.S.
500 population: National Health And Nutrition Examination Survey 1999-2002. *Diabetes Care*
501 **29**, 1263-1268 (2006).
502 5. Unger, R.H., Aguilar-Parada, E., Müller, W.A. & Eisentraut, A.M. Studies of pancreatic alpha
503 cell function in normal and diabetic subjects. *J Clin Invest* **49**, 837-848 (1970).
504 6. Raskin, P., Aydin, I., Yamamoto, T. & Unger, R.H. Abnormal alpha cell function in human
505 diabetes: the response to oral protein. *Am J Med* **64**, 988-997 (1978).
506 7. Raskin, P., Aydin, I. & Unger, R.H. Effect of insulin on the exaggerated glucagon response to
507 arginine stimulation in diabetes mellitus. *Diabetes* **25**, 227-229 (1976).
508 8. D'Alessio, D. The role of dysregulated glucagon secretion in type 2 diabetes. *Diabetes Obes*
509 *Metab* **13 Suppl 1**, 126-132 (2011).
510 9. Cabrera, O.*, et al.* The unique cytoarchitecture of human pancreatic islets has implications
511 for islet cell function. *Proceedings of the National Academy of Sciences* **103**, 2334-2339
512 (2006).
513 10. Cnop, M.*, et al.* The long lifespan and low turnover of human islet beta cells estimated by
514 mathematical modelling of lipofuscin accumulation. *Diabetologia* **53**, 321-330 (2010).
515 11. Drigo, R.A.E.*, et al.* Age Mosaicism across Multiple Scales in Adult Tissues. *Cell Metabolism*
516 **30**, 343-+ (2019).
517 12. Perl, S.*, et al.* Significant human beta-cell turnover is limited to the first three decades of life
518 as determined by in vivo thymidine analog incorporation and radiocarbon dating. *J Clin*
519 *Endocrinol Metab* **95**, E234-239 (2010).
520 13. López-Otín, C., Blasco, M.A., Partridge, L., Serrano, M. & Kroemer, G. Hallmarks of aging: An
521 expanding universe. *Cell* **186**, 243-278 (2023).
522 14. Shrestha, S.*, et al.* Aging compromises human islet beta cell function and identity by
523 decreasing transcription factor activity and inducing ER stress. *Science Advances* **8**,
524 eabo3932 (2022).
525 15. Sandovici, I.*, et al.* Ageing is associated with molecular signatures of inflammation and type
526 2 diabetes in rat pancreatic islets. *Diabetologia* **59**, 502-511 (2016).
527 16. Li, L.*, et al.* Defects in β-cell Ca2+ dynamics in age-induced diabetes. *Diabetes* **63**, 4100-
528 4114 (2014).
529 17. Fontana, L., Partridge, L. & Longo, V.D. Extending healthy life span--from yeast to humans.
530 *Science* **328**, 321-326 (2010).
531 18. Mattison, J.A.*, et al.* Caloric restriction improves health and survival of rhesus monkeys. *Nat*
532 *Commun* **8**, 14063 (2017).
533 19. Green, C.L., Lamming, D.W. & Fontana, L. Molecular mechanisms of dietary restriction
534 promoting health and longevity. *Nat Rev Mol Cell Biol* **23**, 56-73 (2022).
535 20. Anderson, R.M., Le Couteur, D.G. & de Cabo, R. Caloric Restriction Research: New
536 Perspectives on the Biology of Aging. *J Gerontol A Biol Sci Med Sci* **73**, 1-3 (2017).
537 21. Speakman, J.R. & Mitchell, S.E. Caloric restriction. *Mol Aspects Med* **32**, 159-221 (2011).

538 22. Mao, K.*, et al.* Late-life targeting of the IGF-1 receptor improves healthspan and lifespan in
539 female mice. *Nat Commun* **9**, 2394 (2018).
540 23. Liu, G.Y. & Sabatini, D.M. mTOR at the nexus of nutrition, growth, ageing and disease. *Nat*
541 *Rev Mol Cell Biol* **21**, 183-203 (2020).
542 24. Il'yasova, D.*, et al.* Effects of 2 years of caloric restriction on oxidative status assessed by
543 urinary F2-isoprostanes: The CALERIE 2 randomized clinical trial. *Aging Cell* **17**(2018).
544 25. Yang, L., Li, P., Fu, S., Calay, E.S. & Hotamisligil, G.S. Defective hepatic autophagy in obesity
545 promotes ER stress and causes insulin resistance. *Cell Metab* **11**, 467-478 (2010).
546 26. Pyo, J.O.*, et al.* Overexpression of Atg5 in mice activates autophagy and extends lifespan.
547 *Nat Commun* **4**, 2300 (2013).
548 27. Harrison, D.E.*, et al.* Rapamycin fed late in life extends lifespan in genetically
549 heterogeneous mice. *Nature* **460**, 392-395 (2009).
550 28. Martin-Montalvo, A.*, et al.* Metformin improves healthspan and lifespan in mice. *Nat*
551 *Commun* **4**, 2192 (2013).
552 29. Baur, J.A.*, et al.* Resveratrol improves health and survival of mice on a high-calorie diet.
553 *Nature* **444**, 337-342 (2006).
554 30. Chen, C., Liu, Y., Liu, Y. & Zheng, P. mTOR regulation and therapeutic rejuvenation of aging
555 hematopoietic stem cells. *Sci Signal* **2**, ra75 (2009).
556 31. Fraenkel, M.*, et al.* mTOR inhibition by rapamycin prevents beta-cell adaptation to
557 hyperglycemia and exacerbates the metabolic state in type 2 diabetes. *Diabetes* **57**, 945-
558 957 (2008).
559 32. dos Santos, C.*, et al.* Calorie restriction increases insulin sensitivity to promote beta cell
560 homeostasis and longevity in mice. *Nature Communications* **15**, 9063 (2024).
561 33. Matta, L.*, et al.* Chronic intermittent fasting impairs β cell maturation and function in
562 adolescent mice. *Cell Rep* **44**, 115225 (2025).
563 34. Patel, S., Yan, Z. & Remedi, M.S. Intermittent fasting protects β-cell identity and function in a
564 type-2 diabetes model. *Metabolism* **153**, 155813 (2024).
565 35. Brown, M.R.*, et al.* Time-restricted feeding prevents deleterious metabolic effects of
566 circadian disruption through epigenetic control of β cell function. *Sci Adv* **7**, eabg6856
567 (2021).
568 36. Mateus Gonçalves, L., Pereira, E., Werneck de Castro, J.P., Bernal-Mizrachi, E. & Almaça, J.
569 Islet pericytes convert into profibrotic myofibroblasts in a mouse model of islet vascular
570 fibrosis. *Diabetologia* **63**, 1564-1575 (2020).
571 37. Almaca, J.*, et al.* Young capillary vessels rejuvenate aged pancreatic islets. *Proceedings of*
572 *the National Academy of Sciences of the United States of America* **111**, 17612-17617
573 (2014).
574 38. Wright, J.J.*, et al.* Exocrine Pancreas in Type 1 and Type 2 Diabetes: Different Patterns of
575 Fibrosis, Metaplasia, Angiopathy, and Adiposity. *Diabetes* **73**, 1140-1152 (2024).
576 39. Ewald, J.D.*, et al.* HumanIslets.com: Improving accessibility, integration, and usability of
577 human research islet data. *Cell Metab* **37**, 7-11 (2025).
578 40. Kolic, J.*, et al.* Proteomic predictors of individualized nutrient-specific insulin secretion in
579 health and disease. *Cell Metab* **36**, 1619-1633.e1615 (2024).
580 41. Camunas-Soler, J.*, et al.* Patch-Seq Links Single-Cell Transcriptomes to Human Islet
581 Dysfunction in Diabetes. *Cell Metabolism* **31**, 1017-+ (2020).
582 42. Aguayo-Mazzucato, C.*, et al.* Acceleration of beta Cell Aging Determines Diabetes and
583 Senolysis Improves Disease Outcomes. *Cell Metabolism* **30**, 129-+ (2019).

43. Shrestha, S.*, et al.* Aging compromises human islet beta cell function and identity by decreasing transcription factor activity and inducing ER stress. *Science Advances* **8**, 17 (2022).
44. Enge, M.*, et al.* Single-Cell Analysis of Human Pancreas Reveals Transcriptional Signatures of Aging and Somatic Mutation Patterns. *Cell* **171**, 321-330.e314 (2017).
45. Tritschler, S., Theis, F.J., Licked, H. & Bottcher, A. Systematic single-cell analysis provides new insights into heterogeneity and plasticity of the pancreas. *Molecular Metabolism* **6**, 974-990 (2017).
46. Augsornworawat, P., Maxwell, K.G., Velazco-Cruz, L. & Millman, J.R. Single-Cell Transcriptome Profiling Reveals β Cell Maturation in Stem Cell-Derived Islets after Transplantation. *Cell Rep* **32**, 108067 (2020).
47. Chiou, J.*, et al.* Single-cell chromatin accessibility identifies pancreatic islet cell type- and state-specific regulatory programs of diabetes risk. *Nature Genetics* **53**, 455-+ (2021).
48. Bramswig, N.C.*, et al.* Epigenomic plasticity enables human pancreatic α to β cell reprogramming. *J Clin Invest* **123**, 1275-1284 (2013).
49. Avrahami, D.*, et al.* Aging-Dependent Demethylation of Regulatory Elements Correlates with Chromatin State and Improved β Cell Function. *Cell Metabolism* **22**, 619-632 (2015).
50. Avrahami, D.*, et al.* Single-cell transcriptomics of human islet ontogeny defines the molecular basis of β-cell dedifferentiation in T2D. *Mol Metab* **42**, 101057 (2020).
51. Su, C.*, et al.* 3D chromatin maps of the human pancreas reveal lineage-specific regulatory architecture of T2D risk. *Cell Metabolism* **34**, 1394-+ (2022).
52. Arda, H.E.*, et al.* Age-Dependent Pancreatic Gene Regulation Reveals Mechanisms Governing Human beta Cell Function. *Cell Metabolism* **23**, 909-920 (2016).
53. Staels, W.*, et al.* Comprehensive alpha, beta, and delta cell transcriptomics reveal an association of cellular aging with MHC class I upregulation. *Mol Metab* **87**, 101990 (2024).
54. Fasolino, M.*, et al.* Single-cell multi-omics analysis of human pancreatic islets reveals novel cellular states in type 1 diabetes. *Nature Metabolism* **4**, 284-+ (2022).
55. Patil, A.R.*, et al.* Single-cell expression profiling of islets generated by the Human Pancreas Analysis Program. *Nat Metab* **5**, 713-715 (2023).
56. Shapira, S.N., Naji, A., Atkinson, M.A., Powers, A.C. & Kaestner, K.H. Understanding islet dysfunction in type 2 diabetes through multidimensional pancreatic phenotyping: The Human Pancreas Analysis Program. *Cell Metab* **34**, 1906-1913 (2022).
57. Kaestner, K.H., Powers, A.C., Naji, A. & Atkinson, M.A. NIH Initiative to Improve Understanding of the Pancreas, Islet, and Autoimmunity in Type 1 Diabetes: The Human Pancreas Analysis Program (HPAP). *Diabetes* **68**, 1394-1402 (2019).
58. van de Sande, B.*, et al.* A scalable SCENIC workflow for single-cell gene regulatory network analysis. *Nature Protocols* **15**, 2247-2276 (2020).
59. Wu, G. & Haw, R. Functional Interaction Network Construction and Analysis for Disease Discovery. *Methods Mol Biol* **1558**, 235-253 (2017).
60. Zeng, F., Zhang, M.Z., Singh, A.B., Zent, R. & Harris, R.C. ErbB4 isoforms selectively regulate growth factor induced Madin-Darby canine kidney cell tubulogenesis. *Mol Biol Cell* **18**, 4446-4456 (2007).
61. Jin, S.*, et al.* Inference and analysis of cell-cell communication using CellChat. *Nat Commun* **12**, 1088 (2021).
62. Akhmetshina, A.*, et al.* Activation of canonical Wnt signalling is required for TGF-β-mediated fibrosis. *Nat Commun* **3**, 735 (2012).
63. Nguyen, H.N.*, et al.* Leukemia inhibitory factor (LIF) receptor amplifies pathogenic activation of fibroblasts in lung fibrosis. *Proc Natl Acad Sci U S A* **121**, e2401899121 (2024).

632 64. Arbore, G.*, et al.* Complement receptor CD46 co-stimulates optimal human CD8. *Nat*
633 *Commun* **9**, 4186 (2018).
634 65. Hansen, A.S.*, et al.* CD46 is a potent co-stimulatory receptor for expansion of human IFN-γ-
635 producing CD8. *Immunol Lett* **200**, 26-32 (2018).
636 66. Ellingsgaard, H.*, et al.* Interleukin-6 enhances insulin secretion by increasing glucagon-like
637 peptide-1 secretion from L cells and alpha cells. *Nat Med* **17**, 1481-1489 (2011).
638 67. Im, J.Y.*, et al.* DDIAS promotes STAT3 activation by preventing STAT3 recruitment to PTPRM in
639 lung cancer cells. *Oncogenesis* **9**, 1 (2020).
640 68. Dos Santos, C.*, et al.* Caloric restriction promotes beta cell longevity and delays aging and
641 senescence by enhancing cell identity and homeostasis mechanisms. *Res Sq* (2023).
642 69. Duregon, E.*, et al.* Prolonged fasting times reap greater geroprotective effects when
643 combined with caloric restriction in adult female mice. *Cell Metab* **35**, 1179-1194.e1175
644 (2023).
645 70. Mitchell, S.J.*, et al.* Effects of Sex, Strain, and Energy Intake on Hallmarks of Aging in Mice.
646 *Cell Metabolism* **23**, 1093-1112 (2016).
647 71. Pak, H.H.*, et al.* Fasting drives the metabolic, molecular and geroprotective effects of a
648 calorie-restricted diet in mice. *Nature Metabolism* **3**, 1327-+ (2021).
649 72. Spadaro, O.*, et al.* Caloric restriction in humans reveals immunometabolic regulators of
650 health span. *Science* **375**, 671-+ (2022).
651 73. Dos Santos, T.*, et al.* Altered immune and metabolic molecular pathways drive islet cell
652 dysfunction in human type 1 diabetes. *J Clin Invest* (2025).
653 74. Coomans de Brachène, A.*, et al.* Exercise as a non-pharmacological intervention to protect
654 pancreatic beta cells in individuals with type 1 and type 2 diabetes. *Diabetologia* **66**, 450-
655 460 (2023).
656 75. Carapeto, P.*, et al.* Exercise activates AMPK in mouse and human pancreatic islets to
657 decrease senescence. *Nature Metabolism* (2024).
658 76. Al Jobori, H.*, et al.* Empagliflozin Treatment Is Associated With Improved β-Cell Function in
659 Type 2 Diabetes Mellitus. *J Clin Endocrinol Metab* **103**, 1402-1407 (2018).
660 77. Lee, Y.S., Lee, C., Choung, J.S., Jung, H.S. & Jun, H.S. Glucagon-Like Peptide 1 Increases β-
661 Cell Regeneration by Promoting α- to β-Cell Transdifferentiation. *Diabetes* **67**, 2601-2614
662 (2018).
663 78. Hahn, O.*, et al.* A nutritional memory effect counteracts benefits of dietary restriction in old
664 mice. *Nat Metab* **1**, 1059-1073 (2019).
665 79. Kellogg, C.M.*, et al.* Microglial MHC-I induction with aging and Alzheimer's is conserved in
666 mouse models and humans. *Geroscience* **45**, 3019-3043 (2023).
667 80. SantaCruz-Calvo, S.*, et al.* Adaptive immune cells shape obesity-associated type 2
668 diabetes mellitus and less prominent comorbidities. *Nat Rev Endocrinol* **18**, 23-42 (2022).
669 81. Nanaware, P.P.*, et al.* The antigen presentation landscape of cytokine-stressed human
670 pancreatic islets. *Cell Rep* **44**, 115927 (2025).
671 82. Marselli, L.*, et al.* beta-Cell inflammation in human type 2 diabetes and the role of
672 autophagy. *Diabetes Obesity & Metabolism* **15**, 130-136 (2013).
673 83. Jelleschitz, J.*, et al.* Insulitis and aging: Immune cell dynamics in Langerhans islets. *Redox*
674 *Biol* **82**, 103587 (2025).
675 84. De Burghgrave, M.*, et al.* Pancreatic Islet Cells Response to IFNγ Relies on Their Spatial
676 Location within an Islet. *Cells* **12**(2022).
677 85. Avrahami, D.*, et al.* Single-cell transcriptomics of human islet ontogeny defines the
678 molecular basis of beta-cell dedifferentiation in T2D. *Molecular Metabolism* **42**, 14 (2020).

86. Horwitz, E.*, et al.* β-Cell DNA Damage Response Promotes Islet Inflammation in Type 1 Diabetes. *Diabetes* **67**, 2305-2318 (2018).
87. Aguayo-Mazzucato, C.*, et al.* beta Cell Aging Markers Have Heterogeneous Distribution and Are Induced by Insulin Resistance. *Cell Metabolism* **25**, 898-+ (2017).
88. Thompson, P.J.*, et al.* Targeted Elimination of Senescent Beta Cells Prevents Type 1 Diabetes. *Cell Metab* **29**, 1045-1060.e1010 (2019).
89. Dai, X.Q.*, et al.* Heterogenous impairment of alpha cell function in type 2 diabetes is linked to cell maturation state. *Cell Metabolism* **34**, 256-+ (2022).
90. Longo, V.D. & Anderson, R.M. Nutrition, longevity and disease: From molecular mechanisms to interventions. *Cell* **185**, 1455-1470 (2022).
91. Mattison, J.A.*, et al.* Impact of caloric restriction on health and survival in rhesus monkeys from the NIA study. *Nature* **489**, 318-321 (2012).
92. Civitarese, A.E.*, et al.* Calorie restriction increases muscle mitochondrial biogenesis in healthy humans. *PLoS Med* **4**, e76 (2007).
93. da Amaral, M.E.C.*, et al.* Caloric restriction recovers impaired beta-cell-beta-cell gap junction coupling, calcium oscillation coordination, and insulin secretion in prediabetic mice. *American Journal of Physiology-Endocrinology and Metabolism* **319**, E709-E720 (2020).
94. Sheng, C.J.*, et al.* Reversibility of beta-Cell-Specific Transcript Factors Expression by Long-Term Caloric Restriction in db/db Mouse. *Journal of Diabetes Research* **2016**, 11 (2016).
95. Tschen, S.I., Dhawan, S., Gurlo, T. & Bhushan, A. Age-dependent decline in beta-cell proliferation restricts the capacity of beta-cell regeneration in mice. *Diabetes* **58**, 1312-1320 (2009).
96. Ritchie, M.E.*, et al.* limma powers differential expression analyses for RNA-sequencing and microarray studies. *Nucleic acids research* **43**, e47-e47 (2015).
97. Love, M.I., Huber, W. & Anders, S. Moderated estimation of fold change and dispersion for RNA-seq data with DESeq2. *Genome Biol* **15**, 550 (2014).
98. Jin, S., Plikus, M.V. & Nie, Q. CellChat for systematic analysis of cell-cell communication from single-cell transcriptomics. *Nat Protoc* **20**, 180-219 (2025).
99. Hao, Y.*, et al.* Dictionary learning for integrative, multimodal and scalable single-cell analysis. *Nat Biotechnol* **42**, 293-304 (2024).
100. Wang, Y.J.*, et al.* Single-Cell Mass Cytometry Analysis of the Human Endocrine Pancreas. *Cell Metabolism* **24**, 616-626 (2016).
101. Colman, R.J.*, et al.* Caloric restriction delays disease onset and mortality in rhesus monkeys. *Science* **325**, 201-204 (2009).

715 **Figure Legends**

716 **Figure 1 - Aging human islets have an inflammatory activation phenotype combined with**
717 **mTORC1 signaling and elevated unfolded protein response stress. (A)** Islets from young
718 (28±4 years, n=26), and old (71±3 years, n=19) ND donors from the HumanIslets consortium
719 were compared by proteomics. **(B)** Reactome pathways present from significantly abundant pro-
720 teins between young and old ND donors. **(C-G)** Protein expression levels for beta cell immatu-
721 rity marker, RBP4 (C); senescence, CDKN1A/p21 (D); unfolded protein response, CHOP
722 (DDIT3), ATF6, PERK (EIF2AK3) (E); mTORC1 activation, LAMP2, LAMTOR, RAGA, RAGC
723 (F); and immune regulatory components, HLA-A, TGF-β1, TOM1, SLC15A4, CD44, and CD28,
724 respectively (G). HumanIslets, Human Islet Data Analysis and Sharing consortium; HLA, human
725 leukocyte antigen; TCR, T cell receptor; UPR, unfolded protein response. *p<0.05, young vs. old
726 donors. Error bars are mean ± SD.

727 **Figure 2 - Aging increases human alpha cell inflammatory and metabolic signatures. (A)**
728 Age and sex stratification for young (n=11; F=6, M=5) and old (n=21; F=11, M=10) ND donors
729 for scRNA-seq integration, analysis, and SCENIC TF activity. **(B)** Cell type UMAP of integrated
730 scRNA-seq data obtained from HPAP database. **(C)** HLA-ABC expression across endocrine and
731 non-endocrine cell types in human islets. **(D-E)** GSEA hallmarks for gene sets Hallmark Inter-
732 feron Alpha Response (M5911) and Hallmark Interferon GAMMA Response (M5913). **(F)** KEGG
733 hallmarks for Antigen Processing and Presentation by MHC Class I Molecules (M47529). **(G-I)**
734 Significantly expressed Hallmark genes for metabolic processes including Glycolysis (M5937;
735 G), Fatty acid metabolism (M5935; H), and gene ontology pathways for Amino Acid Metabolic
736 Process (GO:0006520; I), respectively. **(J)** Isolated human islet perifusion assay including stim-
737 ulation with amino-acids, glucose, IBMX, and KCL. Dotted line boxes (a', b', and c') highlight
738 specific stimuli that provoked significant glucagon secretion from old islets versus young islets.
739 P-values are shown. Data are mean ± SD with boxplots representing mean ± IQR. Welch's two
740 sample *t-test* was used for panel J, a'-c'. scRNA-seq, single-cell RNA sequencing. TF, transcrip-
741 tion factor; ND, non-diabetic. HPAP, Human Pancreas Analysis Program; GSEA, gene set en-
742 richment analysis.

743 **Figure 3 - Re-wiring of gene regulatory networks activates an inflammatory phenotype in**
744 **aging alpha cells. (A-B)** Gene Regulatory Network (GRN) maps of young (A) and old (B) hu-
745 man alpha cells. Transcription factors (TFs) are represented by white hexagons and inferred TF
746 target genes are shown in solid grey circles. Only the top 15% TF regulons after 100X
747 pySCENIC inference simulations are shown. TF hexagon size represents the TF importance
748 metric within the GRN structure, and TF-target gene nodes are connected by line edges colored
749 using a *viridis* hue to represent predicted connection strength. Disconnected and smaller nodes
750 are shown at the bottom of each GRN network. **(C)** Venn diagrams representing unique and
751 shared genes found in the regulons associated with IRF1, NFKB1, KLF6, MAFB, and HNF1A
752 TFs. **(D)** Regulatory network map displaying age-dependent and age-independent regulatory
753 connections between inflammatory TFs and canonical alpha cell identity TFs. In this map, TFs
754 are represented by solid grey circles and regulatory relationships are shown by arrows. Green
755 arrows, connections found in both young and old alpha cells; dark blue and beige arrows repre-
756 sent connections found uniquely in old and young alpha cells, respectively. **(E-F)** Close up of a
757 Reactome Pathway map displaying significantly enriched pathways associated with genes
758 found in aging alpha cell IRF1, NFKB1, and KLF6 regulons. Different tones of magenta hue rep-
759 resent a false discovery rate (FDR) of at least 0.05 or lower. **(G)** Heatmaps displaying age-de-
760 pendent changes in outgoing ("senders") and incoming ("receivers") cell-cell communication
761 pathways significantly modulated in old islet cells versus young islet cells. Pathway targets were
762 clustered into functional categories (shown x-axis) and their enrichment value for each old cell
763 type (in the y-axis) is shown. Positive values indicate pathways enriched in old islet cells. **(H-I)**

764 Circle plots illustrating growth factor (TGFB1 and FGF) and immune signaling pathways (IL6,
765 CD46) activated in old islets cell types. FGF, IL6, and CD46 were identified as significantly en-
766 riched pathways in old alpha cells. Each cell type is represented by a color and color legend is
767 shown at the bottom.

768 **Figure 4 - Aging increases CD8⁺ islet infiltration via alpha cell MHC-I signaling. (A)** Imag-
769 ing IMC workflow. FFPE pancreatic tissue sections (4-8µm) were labeled simultaneously with 37
770 metal-conjugated antibodies. Laser ablation was conducted for 1,000 x 1,000 µm ROIs selected
771 around islet clusters, and signal quantification was measured by CyTOF. **(B)** UMAPs of subset
772 pancreas cells from all donors, highlighting the islet-endocrine cells (top) and immune cells (bot-
773 tom). **(C)** Representative IMC images and spatial reconstructions of islet-endocrine (top) and
774 islet-immune (bottom) fractions. Scale bar = 100µm **(D)** CODEX workflow and schematic for im-
775 age acquisition and processing of multiplexed datasets generated from 54 markers. **(E)** UMAPs
776 of pancreas cell subsets obtained through CODEX imaging, highlighting endocrine cells (top)
777 and immune subsets (bottom). **(F)** Representative CODEX images and spatial reconstructions
778 for islet endocrine (top) and immune (bottom) subsets. Scale bar = 2000µm. **(G-H)** Immune cell
779 proportions within the total pancreatic immune pool, collected by both IMC (G) and CODEX (H)
780 imaging platforms. **(I)** Density plots illustrating networking distance between CD8⁺ T cells dis-
781 tance and alpha cells, median CD8⁺-alpha cell distance, and the percentage of alpha cells local-
782 ized within ≤50µm of CD8⁺ T cells. **(J)** Density plots showing network distance between CD8⁺ T
783 cells and beta cells, median CD8⁺-beta cell distance, and the percentage of beta cells localized
784 within ≤50µm of CD8⁺ T cells. **(K)** Representative IMC images illustration alpha cells (GCG, red)
785 beta cells (C-peptide, white), and scaled HLA-ABC expression. Scale bar = 100µm. **(L-M)**
786 Quantification of HLA-ABC and HLA-DR intensity from segmented alpha cells (L) and beta cells
787 (M). IMC, imaging mass cytometry; CyTOF, Cytometry by time-of-flight; ROI, region of interest.
788 Welch's two-sample *t-test* was used to compare young and old donors in panels G-J and L-M.
789 Data are mean ± SEM (panels G-J), median ± SEM (L-M).

790 **Figure 5 - T2D expands pancreatic CD8⁺ T-cell populations and shifts islet CD8⁺ T-cell**
791 **states from towards terminal effector-memory phenotypes. (A)** Clinical characteristics ND
792 and T2D adults included for HPAP CODEX imaging. **(B)** UMAP of integrated pancreas samples
793 (942,724 cells) were segmented into immune cells (195,140 cells) and islet endocrine (99,744
794 cells) populations. **(C)** Identified islet endocrine cell populations, including alpha (GCG⁺), beta
795 (C-PEP⁺), "fibrotic" beta cells (C-PEP⁺, COL4A1⁺, COL6⁺), delta (SST⁺), pancreatic polypeptide
796 (PP⁺), and epsilon (ghrelin⁺) cells. **(D)** Scaled beta cell expression of C-PEP, CHGA, NKX6-1
797 and Ki67. **(E)** Scaled alpha cell expression of SOX9 and Ki67. **(F)** Proportions of major pancre-
798 atic immune subsets, including M2-like macrophages (CD163⁺CD68⁺), M1-like macrophages
799 (CD68⁺CD163⁻), granulocytes/monocytes (CD66b⁺), CD8⁺ T cells (CD3⁺CD8⁺), and CD4⁺ T cells
800 (CD3⁺CD4⁺). **(G)** Immune cell density expressed as cells per mm^2. **(H)** CyTOF analysis of islets
801 isolated from young ND (n=12), old ND(n=15), and T2D (n=13) donors. **(I)** Representative gat-
802 ing of viable CD45⁺ immune cells (left) and CD3⁺CD8⁺ T cells (right), sourced from HPAP-164.
803 **(J)** Proportion of CD45⁺ immune cells among viable islet cells (left) and CD3⁺CD8⁺ within the
804 CD45⁺ compartment (right). **(K)** Representative two-parameter (CD27 x CD45RA) plot illustrat-
805 ing CD8⁺ T-cell differentiation states; (1) naïve CD27⁺CD45RA⁺, (2) central memory
806 (CD27⁺CD45RA⁻), 3) and terminal effector memory (CD27⁻CD45RA⁺). **(L)** Distribution of CD8⁺ T
807 cells across naïve CD27⁺CD45RA⁺; $CD8_{naïve}$), central memory (CD27⁺CD45RA⁻; $CD8_{CM}$), and
808 terminal effector memory (CD27⁻CD45RA⁺; $CD8_{TEM}$) phenotypes. **(M)** CD8⁺ T_{EM}/T_{CM} ratio, repre-
809 senting the relative expansion of terminal effector-memory CD8⁺ T cells compared with the cen-
810 tral memory pool. Welch's two sample *t-test* was used for comparisons between pool ND and
811 T2D donors in panels A and C-G. One-way *ANOVA* compared young, old and T2D donors in
812 panels J and L-M. DC, dendritic cell; cDC1, conventional cell; PP, pancreatic polypeptide; NK,

natural killer. *p< 0.05, **p<0.01 for age (old vs. young) and ND vs. T2D groups. Data are mean ± SEM.

Figure 6 - Late-life CR improves glucose tolerance while downregulating alpha cell TCR activation and antigen presentation and processing. (A) 72-week-old C57Bl/6J mice were fed ad-libitum (AL, control) or subjected to 20% calorie restriction (CR) for 2 months. Islets were collected at 80 weeks and processed for IHC and snRNA-seq. **(B)** Percent change in body weight relative to baseline. **(C)** MTTs were performed at baseline (72 weeks) and after the intervention (80 weeks). AUC is presented for each test before and after dietary intervention. **(D)** UMAP of 32,380 islet cells. **(E)** Selected marker genes for endocrine islet subpopulations by scaled gene expression and percent cell expression. **(F)** Number of DEGs affected by CR in endocrine/endothelial cell populations. **(G)** KEGG pathways significantly modified by CR in alpha cells. **(H)** Protein-protein interaction networks predicted from genes downregulated by CR in alpha cells, and subset by 'leukocyte activation' subcluster in red. **(I)** Scaled single-cell expression of MHC class I and II genes in alpha cells. AUC, area under curve; IHC, immunohistochemistry; MTT, mixed meal tolerance test; snRNA-seq, single nucleus RNA sequencing. #p< 0.05 for dietary groups (AL vs. CR); ****p<0.0001 for intervention (Pre- vs. Post-CR).

Figure 7 - Late-life CR attenuates islet adaptive CD8$^+$ effector phenotypes and reduces alpha cell-mediated T-cell recruitment. (A) UMAP of subset immune cell populations (B cells, T cells, macrophages, proliferating B cells, and APCs [dendritic cells] from AL and CR groups. **(B)** Proportion of immune cell populations relative to total islet cells. **(C)** UMAP of T-cell populations from Al and CR groups. **(D)** Proportion of total T cells; * denotes effector CD8$^+$ T cells. **(E)** Expression of Th1-associated genes: *Gzmk*, *Cd25/Il2ra*, *CCr7*, and *Txk*. **(F)** Representative IHC staining for alpha cells (glucagon, red), beta cells (insulin, green) and T cells (CD3, purple). Scale bar = 100µm. **(G)** Pancreatic T-cell density (#CD3$^+$ cells per mm^2). **(H)** T-cell-endocrine cell networks, quantifying the average distance of CD3$^+$ T cells to alpha cells (left), and beta cells (right). **(I)** Intercellular communication networks showing total interaction number relative to interaction signal strength; edge thickness represents relative signal strength. **(J)** Network plot of inferred CD45 signaling interactions. **(K)** Twelve age-matched non-human primates (*Macaca* mulatta) were maintained on AL or 30% CR diets, starting at 7-10 years of age and assessed longitudinally for metabolic outcomes, including peripheral insulin sensitivity via FSIVGTT, until natural death. **(L)** Pancreatic sections (5µm) were stained with H&E and Gomori's Trichrome; islets were manually subset and quantified per image. **(M)** Lipid droplet area, expressed in absolute (#/pancreas) and relative density (#/mm2). **(N)** Trichrome-positive area per islet, subset per primate pancreas and per islet analyzed. H&E, hematoxylin and eosin; FSIVGTT, fasting state intravenous glucose tolerance test. Welch's two sample *t-test* was used for comparisons between AL and CR groups. *p<0.05, ***p<0.001, AL vs. CR. Data are mean ± SEM.

851

852

853

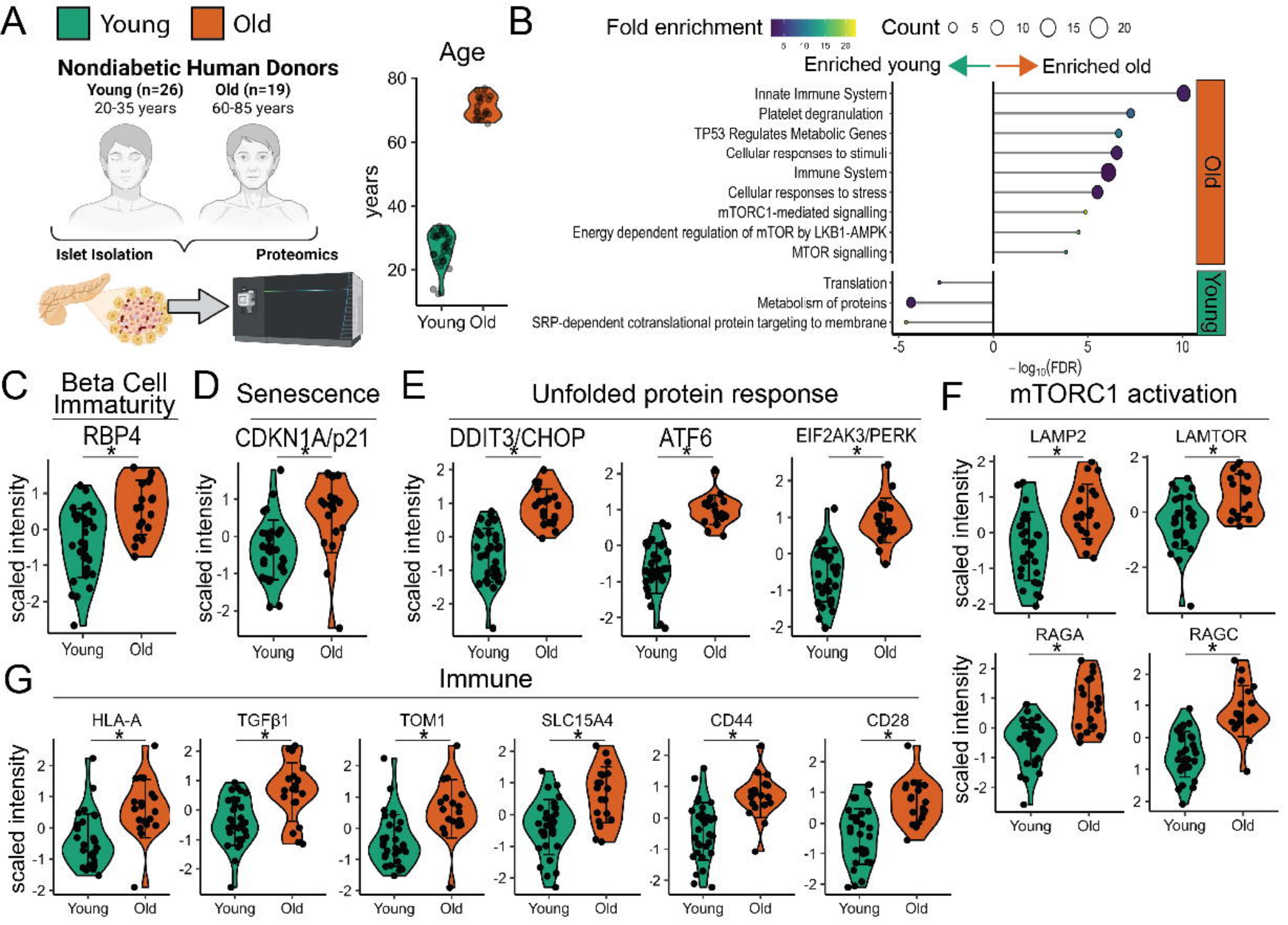
A
Young
Old
Nondiabetic Human Donors
Young (n=26)
20-35 years
Old (n=19)
60-85 years
Islet Isolation
Proteomics
Age
years
Young Old
B
Fold enrichment
Count
Enriched young
Enriched old
Innate Immune System
Platelet degranulation
TP53 Regulates Metabolic Genes
Cellular responses to stimuli
Immune System
Cellular responses to stress
mTORC1-mediated signalling
Energy dependent regulation of mTOR by LKB1-AMPK
MTOR signalling
Translation
Metabolism of proteins
SRP-dependent cotranslational protein targeting to membrane
Old
Young
$-\log_{10}$(FDR)
C
Beta Cell Immaturity
RBP4
D
Senescence
CDKN1A/p21
E
Unfolded protein response
DDIT3/CHOP
ATF6
EIF2AK3/PERK
F
mTORC1 activation
LAMP2
LAMTOR
RAGA
RAGC
G
Immune
HLA-A
TGFβ1
TOM1
SLC15A4
CD44
CD28
scaled intensity
Young
Old

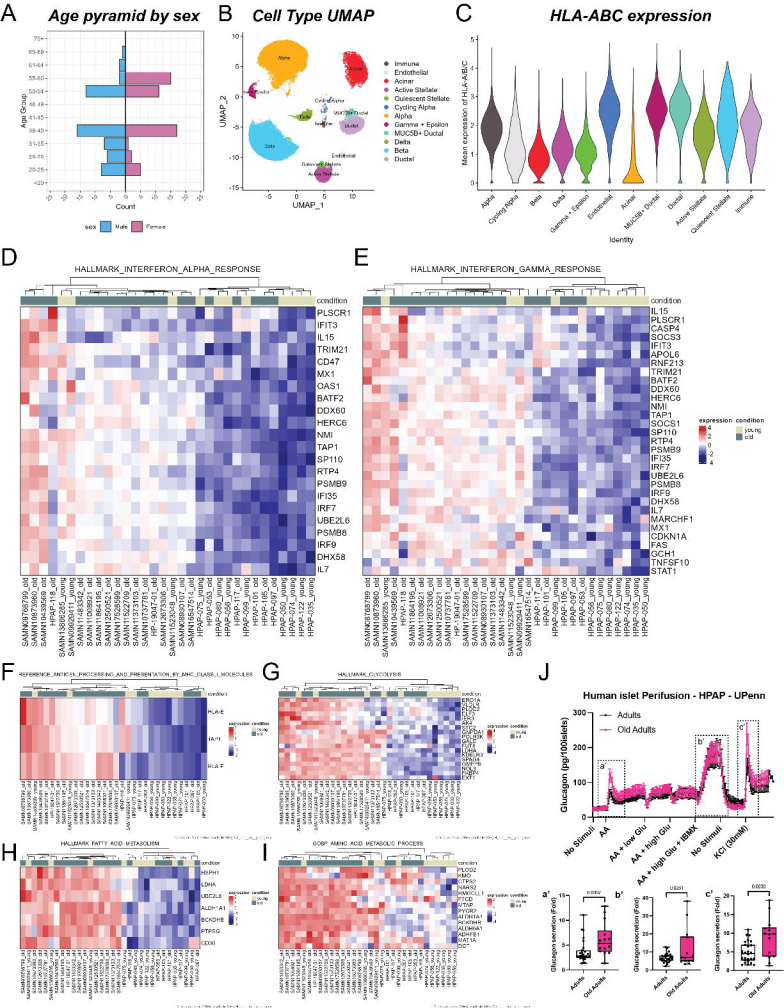
A
Age pyramid by sex
Age Group
Count
sex
Male
Female
B
Cell Type UMAP
UMAP_1
UMAP_2
Immune
Endothelial
Acinar
Active Stellate
Quiescent Stellate
Cycling Alpha
Alpha
Gamma + Epsilon
MUC5B+ Ductal
Delta
Beta
Ductal
C
HLA-ABC expression
Mean expression of HLA-A/B/C
Identity
D
HALLMARK_INTERFERON_ALPHA_RESPONSE
condition
PLSCR1
IFIT3
IL15
TRIM21
CD47
MX1
OAS1
BATF2
DDX60
HERC6
NMI
TAP1
SP110
RTP4
PSMB9
IFI35
IRF7
UBE2L6
PSMB8
IRF9
DHX58
IL7
E
HALLMARK_INTERFERON_GAMMA_RESPONSE
condition
IL15
PLSCR1
CASP4
SOCS3
IFIT3
APOL6
RNF213
TRIM21
BATF2
DDX60
HERC6
NMI
TAP1
SOCS1
SP110
RTP4
PSMB9
IFI35
IRF7
UBE2L6
PSMB8
IRF9
DHX58
IL7
MARCHF1
MX1
CDKN1A
FAS
GCH1
TNFSF10
STAT1
expression
condition
young
old
F
REFERENCE_ANTIGEN_PROCESSING_AND_PRESENTATION_BY_MHC_CLASS_I_MOLECULES
condition
HLA-E
HLA-F
G
HALLMARK_CYCLOCYLISIS
condition
H
HALLMARK_FATTY_ACID_METABOLISM
condition
HSPH1
LDHA
UBC
ALDH1A1
BCKDHB
PTPRG
CD36
I
GOBP_AMINO_ACID_METABOLIC_PROCESS
condition
PLOD2
ALDH1A1
CTPS1
NARS2
SMYD3
PTCD
PTGR
AYSR1
ALDH1A1
HCEHMA
ALDH6A1
ALDH1A1
GATM
PC
J
Human islet Perifusion - HPAP - UPenn
Glucagon (pg/100islets)
Adults
Old Adults
No Stimuli
AA
AA + low Glu
AA + high Glu
AA + high Glu + IBMX
No Stimuli
KCl (30mM)
a'
b'
c'
Glucagon secretion (Fold)
Adults
Old Adults

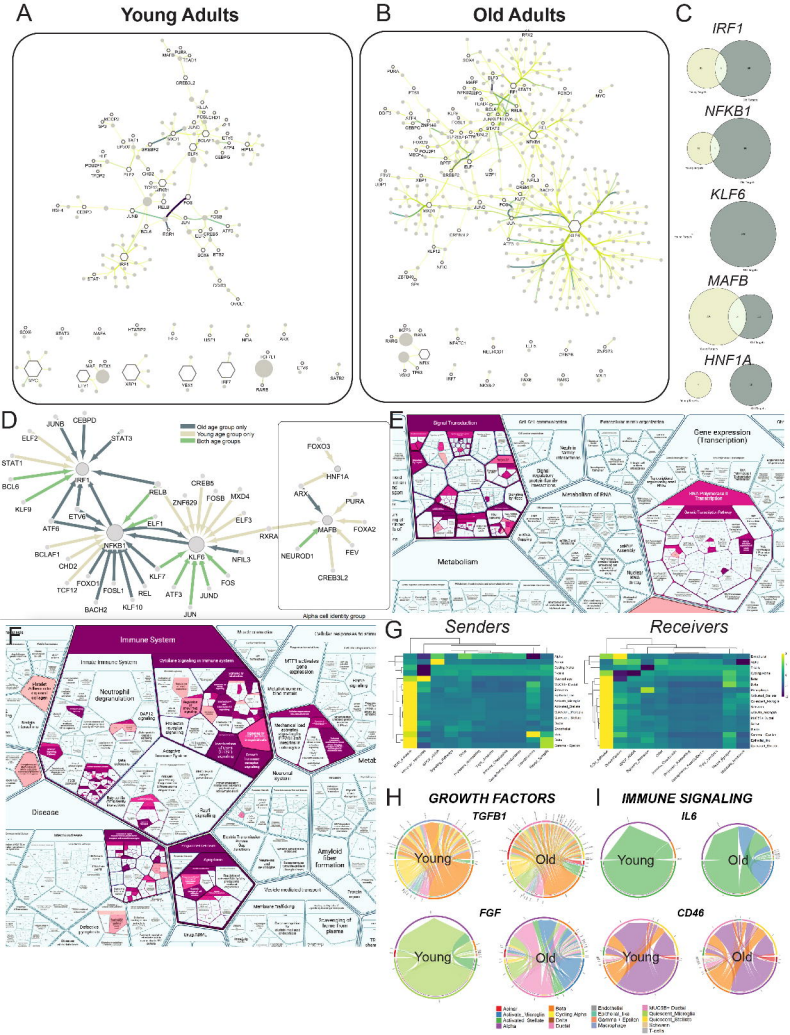
A
Young Adults
B
Old Adults
C
IRF1
NFKB1
KLF6
MAFB
HNF1A
D
Old age group only
Young age group only
Both age groups
JUNB
CEBPD
ELF2
STAT3
STAT1
IRF1
BCL6
KLF9
ETV6
ATF6
RELB
CREB5
FOSB
MXD4
ZNFR29
ELF3
ELF1
NFKB1
BCLAF1
CHD2
FOXD1
TCF12
FOSL1
REL
ATF3
KLF7
KLF10
BACH2
JUN
JUND
FOS
NFIL3
KLF6
RXRA
MAFB
FOXA2
FEV
NEUROD1
CREB3L2
FOXO3
HNF1A
ARX
PURA
Alpha cell identity group
E
Signal Transduction
Metabolism
Gene expression (Transcription)
Metabolism of RNA
F
Immune System
Neutrophil degranulation
Disease
G
Senders
Receivers
H
GROWTH FACTORS
IMMUNE SIGNALING
TGFB1
IL6
FGF
CD46
Young
Old

Imaging Mass Cytometry

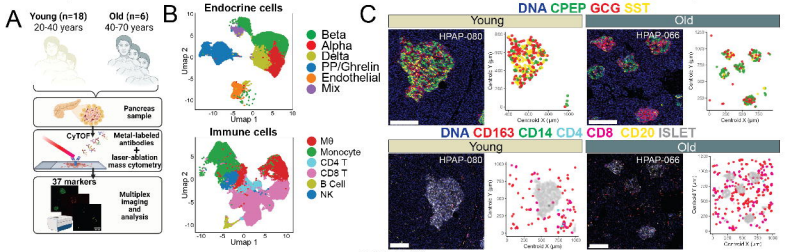

CODEX

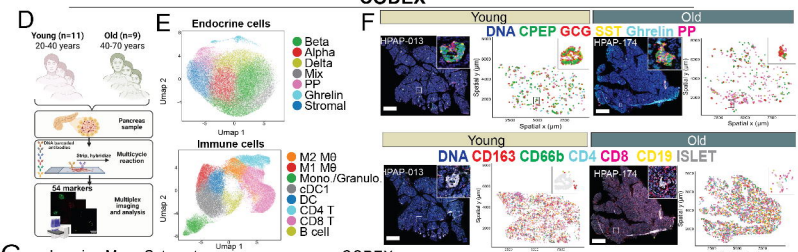

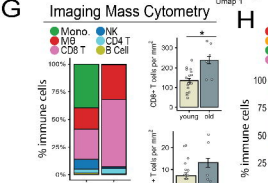

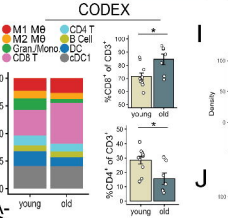

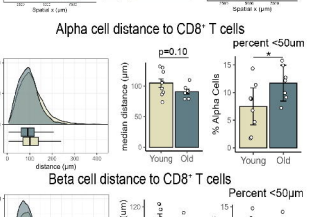

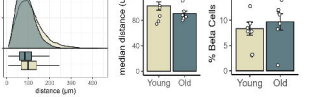

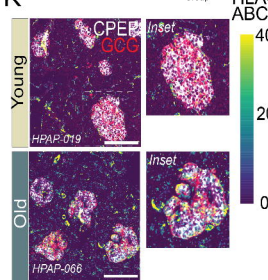

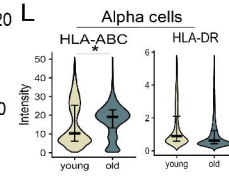

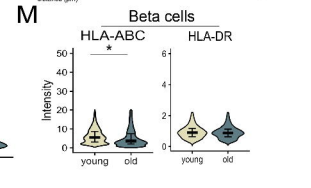

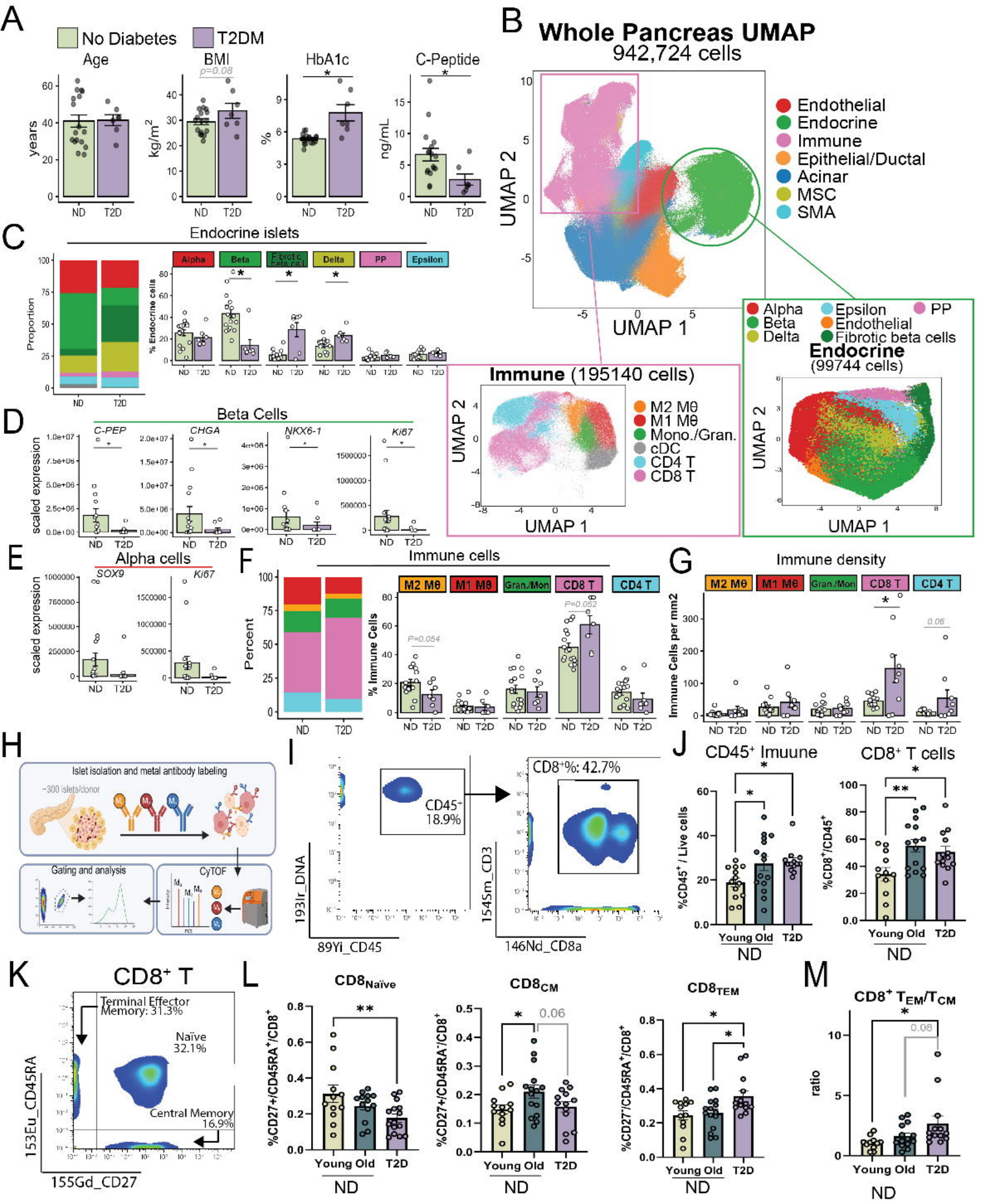
A
No Diabetes
T2DM
Age
BMI
HbA1c
C-Peptide
years
kg/m2
%
ng/mL
p=0.08
ND
T2D
B
Whole Pancreas UMAP
942,724 cells
Endothelial
Endocrine
Immune
Epithelial/Ductal
Acinar
MSC
SMA
UMAP 1
UMAP 2
Immune (195140 cells)
M2 Mθ
M1 Mθ
Mono./Gran.
cDC
CD4 T
CD8 T
Alpha
Beta
Delta
Epsilon
PP
Endothelial
Fibrotic beta cells
Endocrine
(99744 cells)
C
Endocrine islets
Proportion
% Endocrine cells
Alpha
Beta
Fibrotic beta cell
Delta
PP
Epsilon
D
Beta Cells
C-PEP
CHGA
NKX6-1
Ki67
scaled expression
E
Alpha cells
SOX9
Ki67
F
Immune cells
Percent
% Immune Cells
M2 Mθ
M1 Mθ
Gran./Mon
CD8 T
CD4 T
P=0.054
P=0.052
G
Immune density
Immune Cells per mm2
0.06
H
Islet isolation and metal antibody labeling
~300 islets/donor
Gating and analysis
CyTOF
I
CD45+
18.9%
CD8+%: 42.7%
193Ir_DNA
89Yi_CD45
154Sm_CD3
146Nd_CD8a
J
CD45+ Imuune
CD8+ T cells
%CD45+ / Live cells
%CD8+/CD45+
Young Old
T2D
ND
K
CD8+ T
Terminal Effector
Memory: 31.3%
Naïve
32.1%
Central Memory
16.9%
153Eu_CD45RA
155Gd_CD27
L
CD8Naïve
CD8CM
CD8TEM
%CD27+/CD45RA+/CD8+
%CD27+/CD45RA-/CD8+
%CD27-/CD45RA+/CD8+
Young Old
T2D
ND
M
CD8+ TEM/TCM
ratio
0.08
Young Old
T2D
ND

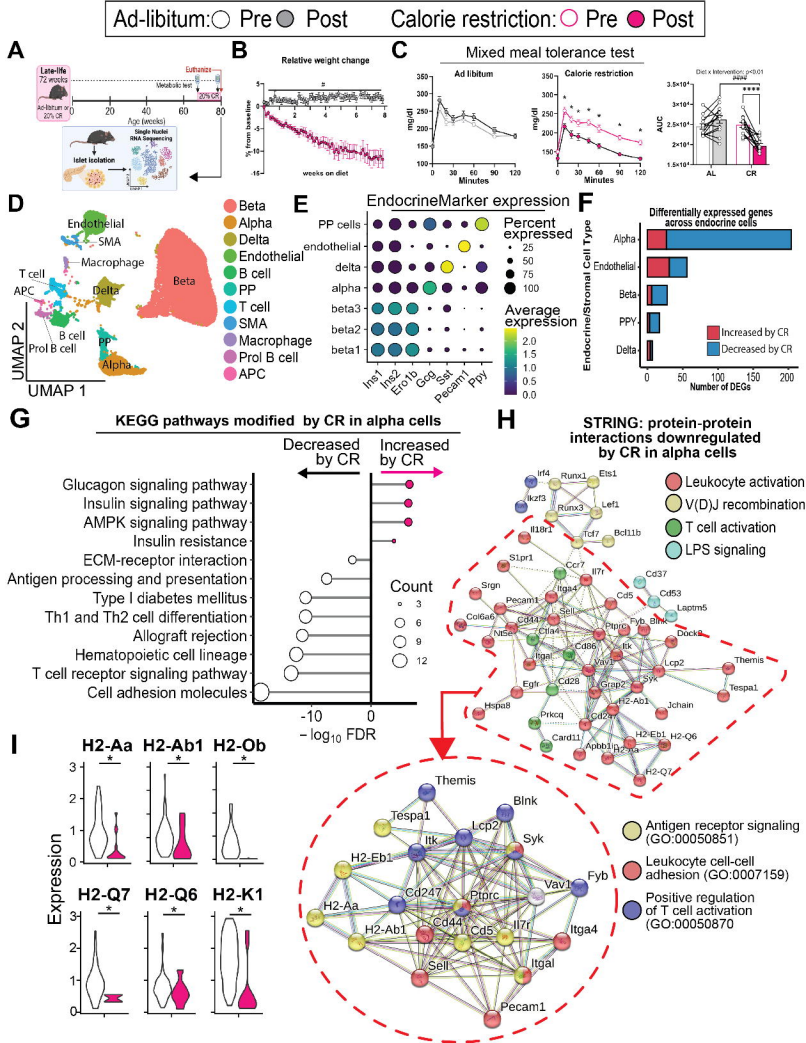

Ad-libitum: Pre Post
Calorie restriction: Pre Post
A
Late-life 72 weeks
Euthanize
Metabolic test
20% CR
Ad-libitum or 20% CR
Age (weeks)
Single Nuclei RNA Sequencing
Islet isolation
B
Relative weight change
% from baseline
weeks on diet
C
Mixed meal tolerance test
Ad libitum
Calorie restriction
mg/dl
Minutes
AUC
AL
CR
D
Endothelial
SMA
Macrophage
T cell
APC
Delta
Beta
B cell
Prol B cell
PP
Alpha
UMAP 2
UMAP 1
Beta
Alpha
Delta
Endothelial
B cell
PP
T cell
SMA
Macrophage
Prol B cell
APC
E
EndocrineMarker expression
PP cells
endothelial
delta
alpha
beta3
beta2
beta1
Ins1
Ins2
Ero1b
Gcg
Sst
Pecam1
Ppy
Percent expressed
25
50
75
100
Average expression
2.0
1.5
1.0
0.5
0.0
F
Differentially expressed genes across endocrine cells
Endocrine/Stromal Cell Type
Alpha
Endothelial
Beta
PPY
Delta
Increased by CR
Decreased by CR
Number of DEGs
G
KEGG pathways modified by CR in alpha cells
Decreased by CR
Increased by CR
Glucagon signaling pathway
Insulin signaling pathway
AMPK signaling pathway
Insulin resistance
ECM-receptor interaction
Antigen processing and presentation
Type I diabetes mellitus
Th1 and Th2 cell differentiation
Allograft rejection
Hematopoietic cell lineage
T cell receptor signaling pathway
Cell adhesion molecules
Count
3
6
9
12
-10
0
– log10 FDR
H
STRING: protein-protein interactions downregulated by CR in alpha cells
Leukocyte activation
V(D)J recombination
T cell activation
LPS signaling
Irf4
Runx1
Ets1
Ikzf3
Runx3
Lef1
Il18r1
Tcf7
Bcl11b
S1pr1
Ccr7
Il7r
Cd37
Srgn
Itga4
Cd5
Cd53
Pecam1
Laptm5
Col6a6
Sell
Cd44
Ptprc
Fyb
Blnk
Nt5e
Ctla4
Dock8
Cd86
Itk
Itgal
Vav1
Lcp2
Themis
Egfr
Cd28
Grap2
Syk
Tespa1
Hspa8
H2-Ab1
Jchain
Prkcq
Cd247
Card11
H2-Eb1
H2-Q6
Apbb1ip
H2-Aa
H2-Q7
Antigen receptor signaling (GO:00050851)
Leukocyte cell-cell adhesion (GO:0007159)
Positive regulation of T cell activation (GO:00050870
I
H2-Aa
H2-Ab1
H2-Ob
H2-Q7
H2-Q6
H2-K1
Expression

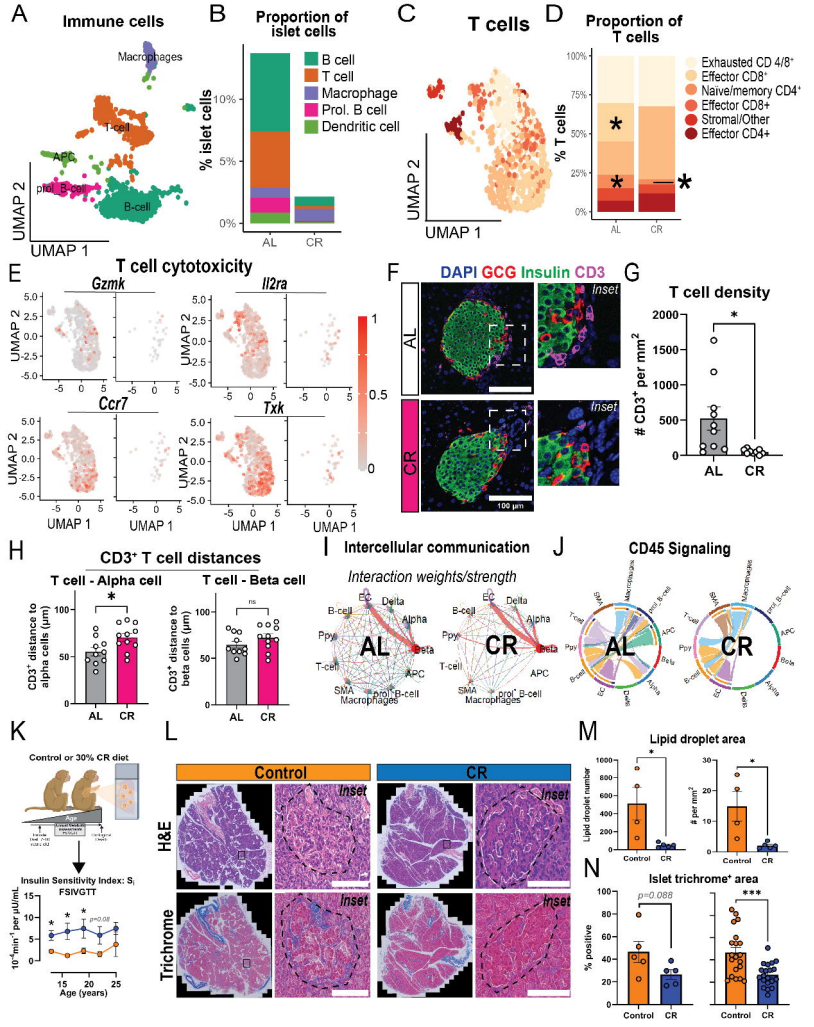
A
Immune cells
Macrophages
T-cell
APC
prol. B-cell
B-cell
UMAP 2
UMAP 1
B
Proportion of islet cells
% islet cells
10%
5%
0%
AL
CR
B cell
T cell
Macrophage
Prol. B cell
Dendritic cell
C
T cells
UMAP 2
UMAP 1
D
Proportion of T cells
% T cells
100%
75%
50%
25%
0%
AL
CR
Exhausted CD 4/8+
Effector CD8+
Naive/memory CD4+
Effector CD8+
Stromal/Other
Effector CD4+
E
T cell cytotoxicity
Gzmk
Il2ra
Ccr7
Txk
UMAP 2
UMAP 1
F
DAPI GCG Insulin CD3
AL
CR
Inset
100 µm
G
T cell density
CD3+ per mm2
2000
1500
1000
500
0
AL
CR
H
CD3+ T cell distances
T cell - Alpha cell
T cell - Beta cell
CD3+ distance to alpha cells (µm)
CD3+ distance to beta cells (µm)
ns
AL
CR
I
Intercellular communication
Interaction weights/strength
AL
CR
EC
Delta
Alpha
Beta
B-cell
Ppy
T-cell
APC
SMA
Macrophages
prol. B-cell
J
CD45 Signaling
AL
CR
SMA
Macrophages
prol. B-cell
APC
Beta
Alpha
Delta
EC
B-cell
Ppy
T-cell
K
Control or 30% CR diet
Age
Insulin Sensitivity Index: SI FSIVGTT
p=0.08
Age (years)
L
Control
CR
H&E
Trichrome
Inset
M
Lipid droplet area
Lipid droplet number
per mm2
Control
CR
N
Islet trichrome+ area
p=0.088
% positive
Control
CR